Optimal-Regulator-Based Control of NPC Boost Rectifiers for Unity Power Factor and Reduced Neutral-Point-Potential Variations

Shoji Fukuda, *Senior Member, IEEE,* Yasumasa Matsumoto, and Akira Sagawa

***Abstract*—Neutral-point-clamped pulsewidth modulation rectifiers (NPCR's) are suitable for high-voltage systems because of their circuit structure. The NPCR's, however, have a problem, in that the neutral point potential (NPP) varies when the current flows into or out of the neutral point. The variations cause voltage deviations in the input waveforms, as well as unbalanced voltage stress on the devices. This paper describes a controlling method for NPCR's based on a state-space model. There are three control objectives: 1) to keep the power factor at unity; 2) to keep the dc-link voltage at a reference value; and 3) to keep the neutral point potential at 0 V. The neutral point current is treated as one of the inputs. The controller is designed based on the optimal regulator theory in order to achieve the three control objectives simultaneously. The validity of the proposed method is demonstrated by experimental results.**

***Index Terms*— Neutral-point-clamped converter, optimal regulator, space-vector-based pulsewidth modulation, state-space model.**

I. Introduction

With the increasing use of high-power static line-side converters, the effects of the harmonic and/or reactive currents generated by these converters are becoming a troublesome problem for the utilities. A voltage-source boost pulsewidth modulation (PWM) rectifier (line-side converter) is promising because it can provide sinusoidal ac currents with unity power factor. Furthermore, it can provide a bilateral power flow.

In this paper, a neutral-point-clamped [1] PWM rectifier (NPCR) is described. An NPCR is suitable for high-power rectifiers because the device voltage stress is one-half of a conventional rectifier, given the same dc-link voltage, and the generated harmonics are less than those generated by a conventional rectifier, given the same switching frequency. Thus, they are expected to play a greater role in high-power applications where device switching is limited below several hundred hertz. However, it has a problem; its neutral point potential (NPP) varies when the current flows into or out of the neutral point [2], thus resulting in an excess voltage stress to either the upper or lower set of the devices. Thus, an NPCR requires an additional control function, namely, the NPP control.

Manuscript received October 29, 1997; revised March 3, 1999. Abstract published on the Internet March 1, 1999.

S. Fukuda is with the Division of Systems and Information, Graduate School of Engineering, Hokkaido University, Sapporo 060-8628, Japan (e-mail: fukus@eng.hokudai.ac.jp).

Y. Matsumoto was with the Division of Systems and Information, Graduate School of Engineering, Hokkaido University, Sapporo 060-8628, Japan. He is now with the Mizusawa Branch, Tohoku Electric Power Company Ltd., Mizusawa 023-0816, Japan.

A. Sagawa is with Design and Development of Traction Systems, Hitachi Company Ltd. Mito Works, Hitachinaka 312-8506, Japan.

Publisher Item Identifier S 0278-0046(99)04132-5.

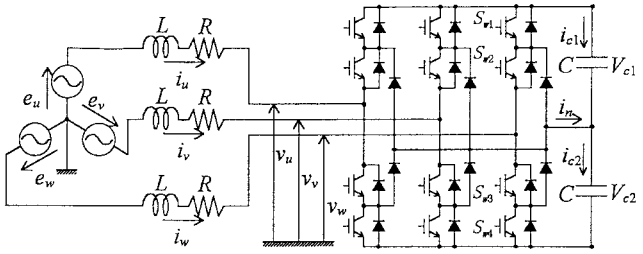

Fig. 1. An NPC voltage-source rectifier.

In this paper, the modeling of an NPCR is carried out and the state equations, which include the NPP, are obtained. An NPCR has three control objectives: 1) to keep the power factor (PF) at unity; 2) to keep the dc-link voltage at a reference value; and 3) to keep the neutral point potential at 0 V. It is shown that an NPCR can be described by a three-input–three-output system. An optimal regulator referred to as a linear quadratic integral (LQI) regulator [3] is used because the regulator is suitable for a multi-input–multi-output system and its stability is insensitive to small parameter variations. The neutral point current, the current flowing into or out of the neutral point, is treated as one of the inputs [4], along with the voltage inputs. Experimental results prove the validity of the proposed modeling and control strategy.

II. Modeling of an NPCR

Fig. 1 shows an NPC voltage-source rectifier, which is the object of this paper. The dc load consists of $R_{\rm dc}$ and $L_{\rm dc}$. The voltages and currents on the ac side are transformed into the d–q coordinate reference frames, which are rotating at the source voltage angular frequency ω. The following equations are obtained:

$$\frac{d}{dt}i_d = -\frac{R}{L}i_d + \omega i_q - \frac{1}{L}v_d + \frac{1}{L}E_1 \tag{1}$$

$$\frac{d}{dt}i_q = -\omega i_d - \frac{R}{L}i_q - \frac{1}{L}v_q \tag{2}$$

where the d and q axes are selected to be $e_d = E_1$, the source line-to-line voltage, and $e_q = 0$. As the instantaneous power

on the ac side is always equal to that on the dc side, the following equation holds [4]:

$$\left.\begin{aligned} v_d i_d + v_q i_q &= V_{c1} i_{c1} + V_{c2} i_{c2} + (V_{c1} + V_{c2}) I_{\rm dc} \\ i_{c1} = C\frac{dV_{c1}}{dt}, \qquad i_{c2} &= C\frac{dV_{c2}}{dt}, \qquad i_{c1} + i_n = i_{c2}. \end{aligned}\right\} \quad (3)$$

Solving (3) for V_{c1} and V_{c2}, we have

$$\frac{d}{dt}V_{c1} = \frac{v_d i_d + v_q i_q - V_{c2} i_n}{C(V_{c1} + V_{c2})} - \frac{I_{\rm dc}}{C} \quad (4)$$

$$\frac{d}{dt}V_{c2} = \frac{v_d i_d + v_q i_q + V_{c1} i_n}{C(V_{c1} + V_{c2})} - \frac{I_{\rm dc}}{C}. \quad (5)$$

The equation in the dc link is

$$\frac{d}{dt}I_{\rm dc} = \frac{V_{c1} + V_{c2}}{L_{\rm dc}} - \frac{R_{\rm dc}}{L_{\rm dc}} I_{\rm dc}. \quad (6)$$

The NPCR is described by (1), (2), and (4)–(6).

III. Control System Design

A. State Equations

There are three control performance criteria for the NPC rectifier, namely, to keep the power factor (PF) at unity, to keep the dc-link voltage at a reference value, and to keep the neutral point potential at 0 V. These conditions are described mathematically as

$$i_q = 0 \quad V_{c1} = V_{c2} = \frac{V_{\rm dc}^*}{2}$$

where $V_{\rm dc}^*$ denotes the reference of the dc-link voltage. The number of control inputs is three: the rectifier input voltages v_d, v_q, and the neutral point current i_n. Thus, the system is a three-input–three-output fifth-order system. As (4) and (5) include nonlinear terms, they must be linearized at an appropriate operating point. The operating point and linearized equations are given in the Appendix. After the linearization, the equations are transformed into a discrete-time system. Modifying the original equations according to the above process, we finally have the state equations as

$$\mathbf{x}(k+1) = \mathbf{A}\mathbf{x}(k) + \mathbf{B}\mathbf{u}(k-1) + \mathbf{E}d(k) \quad (7)$$

where every variable represents a small deviation from the operating point. $\mathbf{u}(k-1)$ represents the input delay caused by a computational time of one sampling period. This is always the case if a microprocessor-controlled system is employed. The output equation is given by

$$\mathbf{y}(k) = \mathbf{C}\mathbf{x}(k). \quad (8)$$

In (7) and (8),

state variable: $\mathbf{x} = [i_d \quad i_q \quad V_{c1} \quad V_{c2} \quad I_{\rm dc}]^T$
input: $\mathbf{u} = [v_d \quad v_q \quad i_n]^T$, *output*: $\mathbf{y} = [i_q \quad V_{c1} \quad V_{c2}]^T$
distrubance: $\mathbf{d} = e_d = E_1$.

B. An Optimal Regulator

It is known that applications of state feedback control are essential for multi-input and multi-output systems. In this paper, an optimal regulator is selected because it guarantees a stable feedback system and is insensitive to small parameter variations. To remove steady-state errors in response to a step reference and/or disturbance change, an integral-type optimal regulator, which is called an LQI regulator [3], is employed.

The objective of an optimal regulator is to find an optimal input that quickly reduces the state variables to zero. Therefore, (7) must be expanded using new state-space variables so as to meet the optimal regulator requirements. Thus, the error system [4]–[6] is applied. The new state variables are the error vector between reference $\mathbf{R}(k)$ and output $\mathbf{y}(k)$, the first-order difference of state vector $\Delta\mathbf{x}(k)$, and the first-order difference of delayed input $\Delta\mathbf{u}(k-1)$. These definitions are

$$\begin{aligned} \mathbf{e}(k) &= \mathbf{R}(k) - \mathbf{y}(k) \\ \Delta\mathbf{x}(k) &= \mathbf{x}(k) - \mathbf{x}(k-1) \\ \Delta\mathbf{u}(k-1) &= \mathbf{u}(k-1) - \mathbf{u}(k-2) \end{aligned}$$

where $\mathbf{R}[i_q^* \;\; V_{c1}^* \;\; V_{c2}^*]^T$ is a reference vector, and $\Delta\mathbf{u}(k-1)$ is introduced as one of the state variables to take into account the output of the delay time of one sampling interval needed for computation. Thus, the augmented state equations in the expanded system are

$$\begin{aligned} \begin{bmatrix} \mathbf{x}_0(k+1) \\ \Delta\mathbf{u}(k) \end{bmatrix} &= \begin{bmatrix} \mathbf{\Phi} & \mathbf{G} \\ \mathbf{0} & \mathbf{0} \end{bmatrix} \begin{bmatrix} \mathbf{x}_0(k) \\ \Delta\mathbf{u}(k-1) \end{bmatrix} + \begin{bmatrix} \mathbf{0} \\ 1 \end{bmatrix} \Delta\mathbf{u}(k) \\ \mathbf{x}_0(k) &= \begin{bmatrix} \mathbf{e}(k) \\ \Delta\mathbf{x}(k) \end{bmatrix} \\ \mathbf{\Phi} &= \begin{bmatrix} \mathbf{I} & -\mathbf{CA} \\ \mathbf{0} & \mathbf{A} \end{bmatrix} \\ \mathbf{G} &= \begin{bmatrix} -\mathbf{CB} \\ \mathbf{B} \end{bmatrix}. \end{aligned} \quad (9)$$

Equation (9) indicates that $\mathbf{x}_0(k)$ and $\Delta\mathbf{u}(k-1)$ approach zero at steady state if the variations in the reference and/or disturbance are stepwise and, then, the LQI regulator requirements are satisfied. This is the reason for introducing the augmented state variables. Equation (9) also indicates that the effects of the input time delay can be taken into account.

The LQI regulator minimizes the following cost function:

$$J = \sum_{k=1}^{\infty} \left\{ [\mathbf{x}_0^T(k) \Delta\mathbf{u}^T(k-1)] \begin{bmatrix} \mathbf{Q} & \mathbf{0} \\ \mathbf{0} & \mathbf{0} \end{bmatrix} \begin{bmatrix} \mathbf{x}_0(k) \\ \Delta\mathbf{u}(k-1) \end{bmatrix} \right\} + \Delta\mathbf{u}^T(k)\mathbf{H}\Delta\mathbf{u}(k) \quad (10)$$

where the diagonal matrices $\mathbf{Q}$ and $\mathbf{H}$ denote the weight for the output and input, respectively. Responses are adjustable by changing the weight values, i.e., larger weights correspond to smaller responses. For example, if a larger value of Q_{id} is chosen, the transient variation in i_d becomes smaller, and vice versa. The weight values are decided by simulation-based examinations of the transient responses.

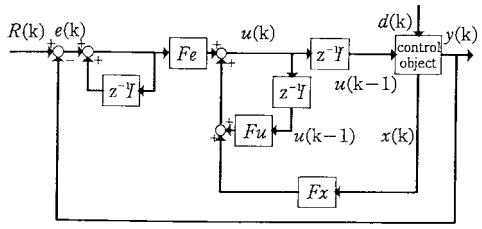

Fig. 2. Control system structure.

TABLE I
SWITCHING STATES AND CORRESPONDING SWITCHING FUNCTION S_i AND INPUT VOLTAGE V_i $(i = u, v, w)$

S_{w1}	S_{w2}	S_{w3}	S_{w4}	S_i	V_i
ON	ON	OFF	OFF	1	V_{c1}
OFF	ON	ON	OFF	0	0
OFF	OFF	ON	ON	-1	V_{c2}

The control input that minimizes the cost function will be given in a feedback form as

$$\mathbf{u}(k) = \mathbf{F}_e \sum_{i=1}^{k} \mathbf{e}(i) + \mathbf{F}_x \mathbf{x}(k) + \mathbf{F}_u \mathbf{u}(k-1) \tag{11}$$

$$[\mathbf{F}_e \quad \mathbf{F}_x \quad \mathbf{F}_u] = -[\mathbf{H} + \mathbf{G}^T \mathbf{P} \mathbf{G}]^{-1} \mathbf{G}^T \mathbf{P} \mathbf{\Phi} (\mathbf{\Phi} \mathbf{G}) \tag{12}$$

where $\mathbf{P}$ is the semidefinite matrix which satisfies the following Riccati equation [3]:

$$\mathbf{P} = \mathbf{Q} + \mathbf{\Phi}^T \mathbf{P} \mathbf{\Phi} - \mathbf{\Phi}^T \mathbf{P} \mathbf{G} [\mathbf{H} + \mathbf{G}^T \mathbf{P} \mathbf{G}]^{-1} \mathbf{G}^T \mathbf{P} \mathbf{\Phi}. \tag{13}$$

Equation (11) clearly indicates that a servo system of 1-type with integral compensation can be constructed, as shown in Fig. 2.

IV. PWM PATTERN CREATION PRINCIPLE

Here, a PWM pulse pattern creation method which can realize an arbitrary control input given by the LQI regulator is presented.

A. Instantaneous Space Vector

The switching function, S_i $(i = u, v, w)$, is defined in Table I. The definition of the instantaneous space vector V_k is given by

$$\mathbf{V}_k = v_u + v_v e^{j\frac{2\pi}{3}} + v_w e^{j\frac{4\pi}{3}} \quad \text{where } v_i = S_i V_i, \qquad i = u, v, w. \tag{14}$$

The input potential of the rectifier, v_u, v_v, v_w, takes on three values, V_{c1}, 0, and $-V_{c2}$. Thus, there are 27 switching modes corresponding to each of the three-phase switching states (S_u, S_v, S_w).

If the NPP is maintained at 0 V, which means $V_{c1} = V_{c2}$, then there are 19 space vectors. They are shown by the apexes of the small triangles in Fig. 3. The largest ones, $\mathbf{V}_1 - \mathbf{V}_6$, are called LL-vectors; the second largest ones, $\mathbf{V}_{12} - \mathbf{V}_{61}$, are called L-vectors; the ones reduced by a factor of two, $\mathbf{V}_{01} - \mathbf{V}_{06}$, are called half (HF) vectors; and the zero vector is $\mathbf{V}_0$. There are two kinds of HF-vectors, e.g., $\mathbf{V}_{01}$ of $(1,0,0)$ and of $(0,-1,-1)$. Both vectors produce the same line voltages as far as $\mathbf{V}_{c1} = \mathbf{V}_{c2}$, but produce different phase voltages. The former is called a positive HF vector and is specified as $\mathbf{V}_{01p}$, because it provides positive zero-sequence voltage, and the latter is called a negative HF vector, and is specified as $\mathbf{V}_{01n}$, because it provides negative zero-sequence voltage. The HF-vectors are very important in controlling the NPP because if the output of $\mathbf{V}_{01p}$ results in a decrease in the NPP for one sampling interval, the output of $\mathbf{V}_{01n}$ results in an increase in the NPP for the same sampling interval, and vice versa. There are three kinds of zero vectors, $\mathbf{V}_0$ $(1,1,1)$, $(0,0,0)$, and $(-1,-1,-1)$.

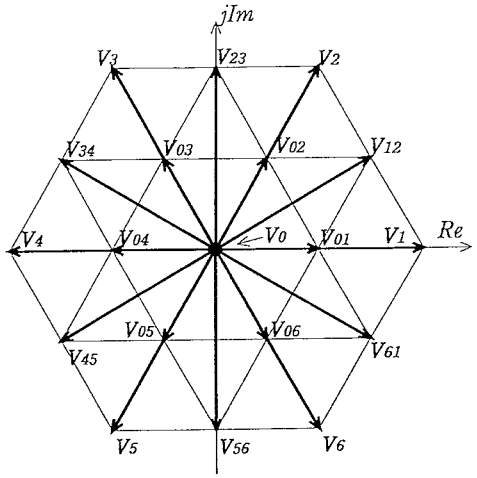

Fig. 3. Space vectors generated by NPCR.

The reference input voltages should be represented in the space-vector form. When input voltages v_d and v_q are given by $\mathbf{u}(k)$ in (11), they are transformed into the d and q components of the modulation index [5], [7] as

$$M_d = \frac{\sqrt{2} v_d}{V_{c1} + V_{c2}}, \qquad M_q = \frac{\sqrt{2} v_q}{V_{c1} + V_{c2}}. \tag{15}$$

Then, the modulation index M and the phase angle ϕ are given by

$$M = \sqrt{M_d^2 + M_q^2}, \qquad 0 \le M \le 1 \tag{16}$$

$$\phi = \omega t + \delta, \qquad \delta = \tan^{-1}\left(\frac{M_q}{M_d}\right). \tag{17}$$

B. Pulsewidth Calculation

Let the input reference voltage represented by the space vector be

$$\mathbf{V}_r = \frac{\sqrt{3}}{2} V_{\mathrm{dc}} M e^{j\phi}, \qquad V_{\mathrm{dc}} = V_{c1} + V_{c2}. \tag{18}$$

Consider the case where $\mathbf{V}_r$ exists in the range $0 \le \phi \le \pi/3$, where ϕ hereafter is measured from the real axis. The range $0 \le \phi \le \pi/3$ is divided into four small triangular regions, 1, 2, 3, and 4, as shown in Fig. 4. The principle of PWM control is that the reference vector $\mathbf{V}_r$ is approximated by using three

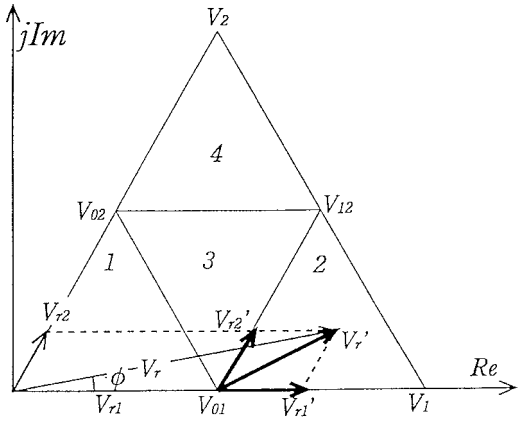

Fig. 4. Reference vector $\mathbf{V}_r'$ in space-vector notation for $0 \le \varphi \le \pi/3$.

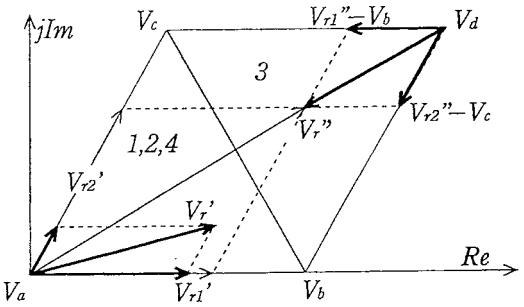

Fig. 5. Decomposition of reference vector $\mathbf{V}_r'$ into three space vectors to calculate pulsewidths.

adjacent vectors represented by the three apexes of one of the four triangles; the vectors $\mathbf{V}_{01}$, $\mathbf{V}_1$, and $\mathbf{V}_{12}$ are used if $\mathbf{V}_r$ is located in region 2, as is the case in Fig. 4. The region where $\mathbf{V}_r$ exists can be identified if $\mathbf{V}_{r1}$ and $\mathbf{V}_{r2}$ are compared to the side length, V $(=V_{\rm dc}/2)$, of the small triangle. Decomposing $\mathbf{V}_r$ into the two directions, $\mathbf{V}_1$ and $\mathbf{V}_2$ in Fig. 4, we have

$$\left.\begin{aligned} \mathbf{V}_r &= \mathbf{V}_{r1} + \mathbf{V}_{r2} \\ \mathbf{V}_{r1} &= \tfrac{V_{\rm dc}}{2} M(\sqrt{3}\cos\phi - \sin\phi) \\ \mathbf{V}_{r2} &= V_{\rm dc} M \sin\phi. \end{aligned}\right\} \tag{19}$$

Region 2 of Fig. 4 is enlarged in Fig. 5, where the apexes of the triangle can be rewritten as $\mathbf{V}_{01} = \mathbf{V}_a$, $\mathbf{V}_{12} = \mathbf{V}_c$, and $\mathbf{V}_1 = \mathbf{V}_b$. Also, the new reference vector $\mathbf{V}_r'$ is defined on the basis of the new origin $\mathbf{V}_a$, as shown in Fig. 5. Decompose $\mathbf{V}_r'$ into $\mathbf{V}_{r1}'$ and $\mathbf{V}_{r2}'$, and define the normalized voltages as

$$x = \frac{2V_{r1}'}{V_{\rm dc}} \quad y = \frac{2V_{r2}'}{V_{\rm dc}}.$$

The normalized output times for each of the three vectors $\mathbf{V}_b$, $\mathbf{V}_c$, and $\mathbf{V}_a$ are

$$\alpha_b = x \quad \alpha_c = y \quad \alpha_a = 1 - \alpha_b - \alpha_c \tag{20}$$

respectively. The same procedure for obtaining the normalized output times is applicable if $\mathbf{V}_r$ is located in regions 1 and 4.

If $x + y > 1$, $\mathbf{V}_r$ will exist in region 3. In this special case, $\mathbf{V}_d$ is selected as the new origin instead of $\mathbf{V}_a$, as shown in Fig. 5. Thus, the normalized output times for $\mathbf{V}_b$, $\mathbf{V}_c$, and $\mathbf{V}_d$ are, in this case,

$$\alpha_b = 1 - x \quad \alpha_c = 1 - y \quad \alpha_d = 1 - \alpha_b - \alpha_c \tag{21}$$

respectively. The actual timewidth for the output vectors is the product of α's and the sampling interval T.

TABLE II
OUTPUT SEQUENCE OF VOLTAGE VECTORS

Location of V_r	Output Sequence
Region 1 for $0<\phi<\pi/6$	$V_{01p}\rightarrow V_{00}\rightarrow V_{01n}\rightarrow V_{01n}$
$\pi/6<\phi<\pi/3$	$V_{02p}\rightarrow V_{01p}\rightarrow V_{00}\rightarrow V_{02n}$
Region 2	$V_{01p}\rightarrow V_{12}\rightarrow V_{1}\rightarrow V_{01n}$
Region 3 for $0<\phi<\pi/6$	$V_{01p}\rightarrow V_{12}\rightarrow V_{02n}\rightarrow V_{01n}$
$\pi/6<\phi<\pi/3$	$V_{02p}\rightarrow V_{01p}\rightarrow V_{12}\rightarrow V_{02n}$
Region 4	$V_{02p}\rightarrow V_{2}\rightarrow V_{12}\rightarrow V_{02n}$

C. Output Sequence of Voltage Vectors

In order to decide the output sequence of voltage vectors, the following conditions must be considered [8]:

1) the sequence for which one of the input variables, i_n, is controllable;
2) the sequence under which a single switching enables us to change one vector to the following vector.

Suppose that a reference $\mathbf{V}_r$ is located in region 2, as shown in Fig. 4. The vectors $\mathbf{V}_{01}$, $\mathbf{V}_{12}$, and $\mathbf{V}_1$ are used in this case because they satisfy condition 2). The timewidth during which each vector is used is given by (20), e.g., α_a provides the normalized time for the HF-vector $\mathbf{V}_{01}$. Each HF-vector has two kinds; $\mathbf{V}_{01p}$ as well as $\mathbf{V}_{01n}$ can be output for an arbitrary time duration as far as the sum of each output time equals to α_a. If the output of $\mathbf{V}_{01p}$ results in a decrease in the NPP for one sampling interval, the output of $\mathbf{V}_{01n}$ results in an increase in the NPP for the same sampling interval. Thus, the ratio of the output time of $\mathbf{V}_{01p}$ to $\mathbf{V}_{01n}$ varies the NPP. This is the control principle of the NPP.

In the three different vectors used for one sampling interval, the same HF vector is used as the first and last vectors, but if the first one is a positive HF-vector, then the last one must be a negative HF-vector, and vice versa. Thus, the output sequence of voltage vectors in this case is

$$\mathbf{V}_{01p} \rightarrow \mathbf{V}_{12} \rightarrow \mathbf{V}_1 \rightarrow \mathbf{V}_{01n}.$$

For the next sampling interval, the reverse sequence of output vectors is used to assure symmetrical operation. The output sequence of voltage vectors for the other regions is summarized in Table II [8].

D. NPP Control Method

Define the switching function related to the NPP for phase w as

$$\begin{aligned} S_{nw} &= 1, \qquad \text{when } S_w = 0 \\ &= 0, \qquad \text{when } S_w = 1 \text{ or } -1. \end{aligned}$$

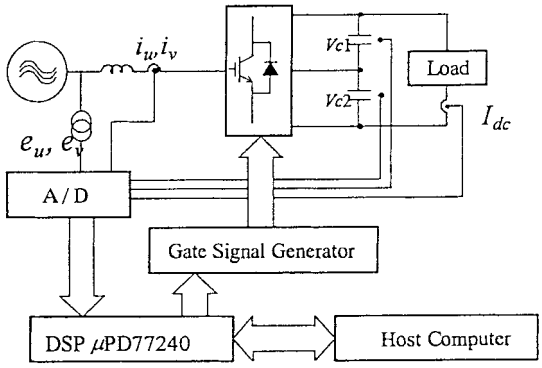

Fig. 6. Configuration of NPCR controller.

If $S_{nw} = 1$, both the switches S_{w2} and S_{w3} in Fig. 1 are triggered. Then, the current i_w flows into or out of the neutral point, namely, i_w flows into the neutral point if $i_w > 0$, and i_w flows out of the neutral point if $i_w < 0$. One sampling interval can be divided into four subintervals corresponding to each of the four kinds of vectors used for the sampling interval. Then, the current flowing into the neutral point at the jth subinterval, i_{nj}, is given by

$$i_{nj} = S_{nuj} i_u + S_{nvj} i_v + S_{nwj} i_w, \qquad j = 1, 2, 3, 4. \quad (22)$$

If currents are assumed to be constant during a sampling interval, which is the case in discrete-time systems, the average neutral point current over one sampling interval, i_n, will be given by

$$i_n = \alpha_1 i_{n1} + \alpha_2 i_{n2} + \alpha_3 i_{n3} + \alpha_4 i_{n4} \quad (23)$$

where $\alpha_1 - \alpha_4$ represent the normalized times during which each of the four kinds of input vectors is used for one sampling interval, and $i_{n1} - i_{n4}$ are the neutral point currents provided by each of the four vectors. Equations (22) and (23) indicate that the value of i_n depends on the magnitude of three phase currents, i_u, i_v, and i_w, and the timewidths, $\alpha_1 + \alpha_4$, α_2, and α_3. Therefore, an arbitrarily large amount of i_n cannot be provided during one sampling period. If an excessive amount of i_n is required by the regulator, it must be provided over several sampling intervals.

According to the output vector sequence shown in Table II, the first and last vectors are the same HF-vector, but one is positive and the other is negative. Considering the fact that $i_u + i_v + i_w = 0$, we have

$$i_{n1} + i_{n4} = 0. \quad (24)$$

Establish the normalized times during which a positive and a negative HF-vector are used as

$$\alpha_p = \frac{\alpha}{2}(1 + r) \quad \alpha_n = \frac{\alpha}{2}(1 - r) \quad (25)$$

respectively, where α $(= \alpha_1 + \alpha_4)$ is the total timewidth for the HF-vector. The variable r takes on the value $-1 \le r \le 1$. Substituting (25) into (23), we have

$$r = \frac{i_n - \alpha_2 i_{n2} - \alpha_3 i_{n3}}{\alpha i_{n1}}. \quad (26)$$

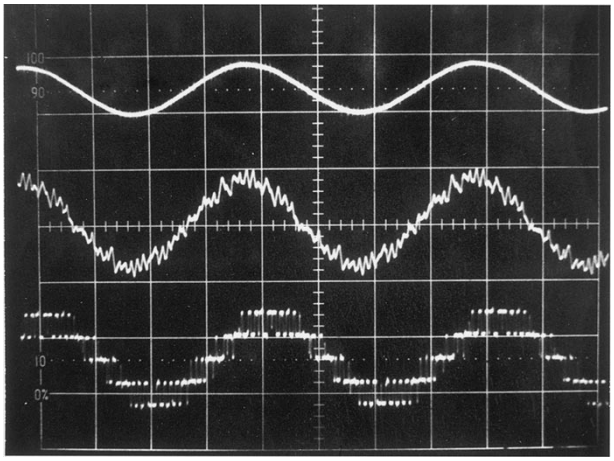

(a)

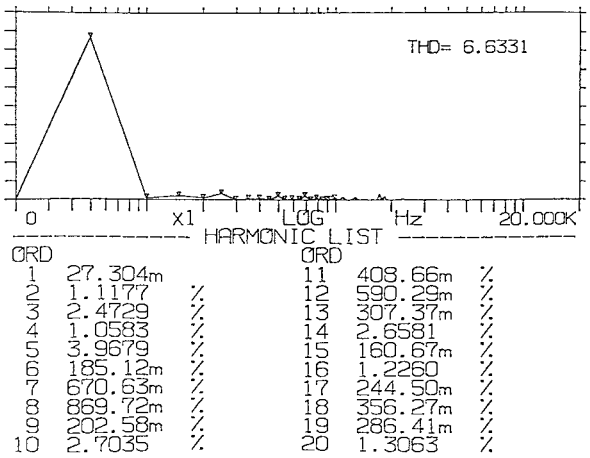

(b)

Fig. 7. (a) Voltage and current waveforms in steady state. Upper trace: e_u, 200 V/div. Middle trace: i_u, 10 A/div. Lower trace: v_{wu}, 200 V/div, 5 ms/div. (b) Harmonic spectrum for i_u.

Substitution of the required control input i_n into (26) gives us the time ratio r, which will produce i_n. However, it should be noted that the required amount of neutral point current i_n may not be provided in one sampling interval because r is limited. Slower NPP responses will result in this situation.

V. Experimental Results

The experiments [9] were carried out under the following conditions: ac source voltage, $E_1 = 100$ V; ac reactor, $L = 5$ mH; $R = 0.4\ \Omega$; dc capacitor, $C = 500\ \mu$F; and dc load, $L_{\rm dc} = 5$ mH, $R_{\rm dc} = 52\ \Omega$, or $32\ \Omega$. The references were $V_{c1}^* = V_{c2}^* = 80$ V and $i_q^* = 0$ A. The sampling frequency was 1800 Hz. The average switching frequency of the devices was below 500 Hz, thus indicating that high-power gate-turn-off thyristors (GTO's) may be applicable.

Fig. 6 shows the configuration of the NPCR controller used for experiments. A digital signal processor (NEC, μP77240) executes algorithms such as the coordinate transformation, input calculation, and PWM signal generation to the rectifier. Voltage and current waveforms at steady state and the harmonic spectrum for input current are shown in Fig. 7(a)

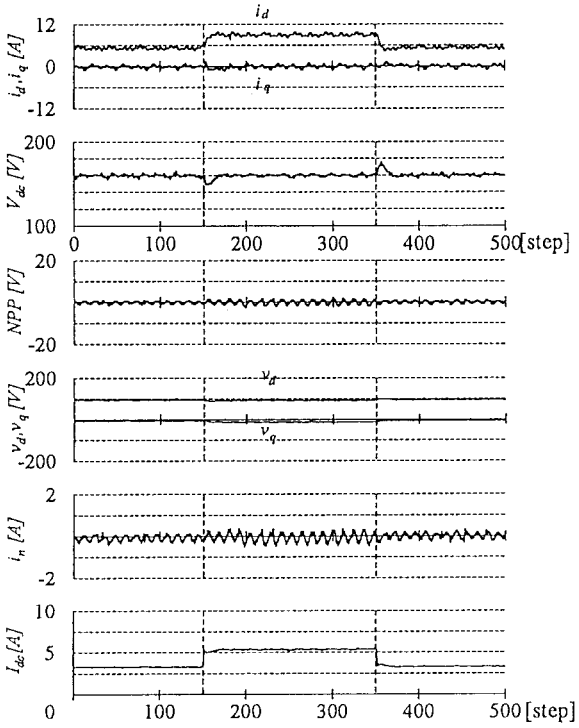

Fig. 8. Responses to step changes in a load resistance $R_{\rm dc} = 52\ \Omega \rightarrow 32\ \Omega \rightarrow 52\ \Omega$; 55.5 ms (100 steps)/div.

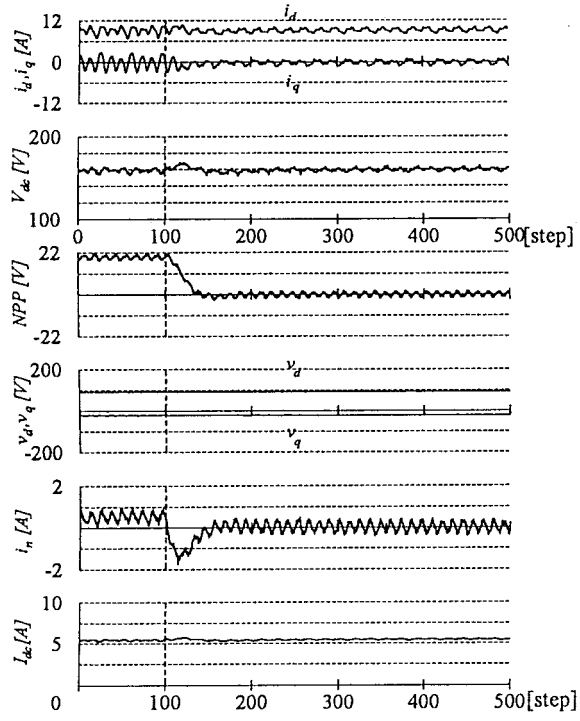

Fig. 9. Responses to a step change in an NPP reference. $\mathrm{NPP} = 20\ \mathrm{V} \rightarrow 0\ \mathrm{V}$; 55.5 ms (100 steps)/div.

and (b), respectively. We can observe that the input current is almost sinusoidal with unity power factor.

Responses to the parameter variations are shown in Fig. 8, where the load resistance $R_{\rm dc}$ was changed in a stepwise fashion from $R_{\rm dc} = 52\ \Omega$ to $32\ \Omega$ in 150 steps, and then back

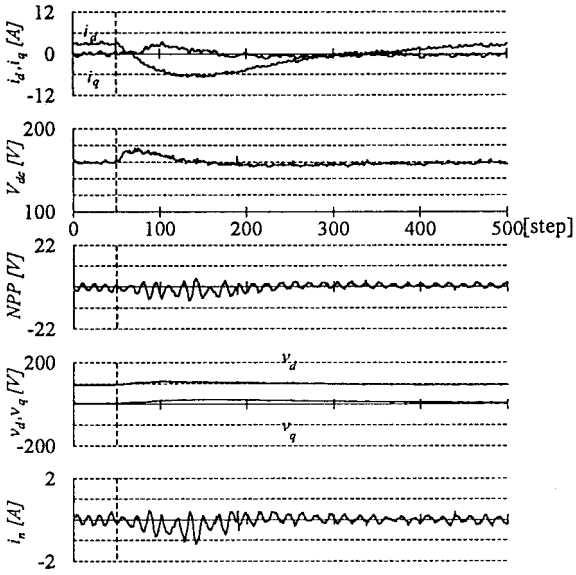

Fig. 10. Responses to a step change in an inverter frequency. $f_i = 40 \rightarrow 37.5$ Hz; 55.5 ms (100 steps)/div.

to 52 Ω in 350 steps where 100 sampling steps $= 55.5$ ms. We have confirmed that the system is stable when subjected to load variations, which suggests that a robust control system has been obtained, and the control purposes have been achieved.

Fig. 9 shows the effects of the NPP control. The NPP reference was initially set at NPP $= 20$ V ($V_{c1} = 100$ V, $V_{c2} = 60$ V). The NPP reference was then changed to NPP $= 0$ V at 100 steps. We can observe that the NPP approaches zero in a stable fashion, which indicates that if there is a deviation in the NPP for some reason, it will eventually be forced to zero. As the maximum value for the current flowing into the neutral point for one sampling period, i_n, is limited, the response time for the NPP control is relatively slow. The required i_n is provided over several sampling periods in this situation.

An induction motor drive was successfully tested. The dc load, $R_{\rm dc}$ and $L_{\rm dc}$, was removed and a three-phase NPC inverter was connected to the dc link to feed a 1-kW induction motor. Responses when an inverter output frequency was changed from 40 to 37.5 Hz at 50 steps are shown in Fig. 10, where f/V was kept constant. We can observe that i_d becomes negative shortly after the frequency change and then slowly back to a positive value, which suggests that regenerative operation has been performed.

VI. Conclusion

In this paper, the modeling and control of an NPC three-phase voltage-source boost rectifier have been carried out. The neutral point current is treated as one of the inputs. The linear state equations obtained from the analysis are useful for designing a state feedback control system.

The relation between the neutral point current and the half vectors used is clarified. The method of controlling the NPP by adjusting the output time ratio of a positive half vector to a negative half vector is employed. An integral-type optimal regulator is used for the rectifier control. The regulator enables us not only to accomplish three control purposes,

$$\mathbf{A}_c = \begin{bmatrix} -\frac{R}{L} & \omega & 0 & 0 & 0 \\ -\omega & -\frac{R}{L} & 0 & 0 & 0 \\ \frac{v_{d0}}{C(V_{c10}+V_{c20})} & \frac{v_{q0}}{C(V_{c10}+V_{c20})} & -\frac{1}{CR_{\rm dc}} & -\frac{1}{CR_{\rm dc}} & -\frac{1}{C} \\ \frac{v_{d0}}{C(V_{c10}+V_{c20})} & \frac{v_{q0}}{C(V_{c10}+V_{c20})} & -\frac{1}{CR_{\rm dc}} & -\frac{1}{CR_{\rm dc}} & -\frac{1}{C} \\ 0 & 0 & \frac{1}{L_{\rm dc}} & \frac{1}{L_{\rm dc}} & -\frac{R_{\rm dc}}{L_{\rm dc}} \end{bmatrix}$$

$$\mathbf{B}_c = \begin{bmatrix} -\frac{1}{L} & 0 & 0 \\ 0 & -\frac{1}{L} & 0 \\ \frac{i_{d0}}{C(V_{c10}+V_{c20})} & \frac{i_{q0}}{C(V_{c10}+V_{c20})} & -\frac{1}{2C} \\ \frac{i_{d0}}{C(V_{c10}+V_{c20})} & \frac{i_{q0}}{C(V_{c10}+V_{c20})} & \frac{1}{2C} \\ 0 & 0 & 0 \end{bmatrix}$$

$$\mathbf{C} = \begin{bmatrix} 0 & 1 & 0 & 0 & 0 \\ 0 & 0 & 1 & 0 & 0 \\ 0 & 0 & 0 & 1 & 0 \end{bmatrix}$$

$$\mathbf{E}_c = \begin{bmatrix} \frac{1}{L} & 0 & 0 & 0 & 0 \end{bmatrix}^T$$

namely, PF control, NPP control, and dc-link voltage control simultaneously, but to realize a stable system in the event of load variations. The validity of the modeling and the control strategy is confirmed by experimental results.

APPENDIX

The operating points identified by the subscript "0" are

$$\begin{aligned} i_{q0} &= 0 \\ v_{d0} &= E_1 \\ i_{n0} &= 0 \\ I_{\rm dc0} &= \frac{V_{c10}+V_{c20}}{R_{\rm dc}} \\ i_{d0} &= \frac{E_1 - \sqrt{E_1^2 - 4R(V_{c10}+V_{c20})I_{dc0}}}{2R} \\ v_{d0} &= E_1 - Ri_{d0} \\ v_{q0} &= -\omega L i_{d0}. \end{aligned}$$

Linearizing (1), (2), and (4)–(6) around the operating points, a state equation of the following form is obtained:

$$\frac{d}{dt}\mathbf{x} = \mathbf{A}_c\mathbf{x} + \mathbf{B}_c\mathbf{u} + \mathbf{E}_c\mathbf{d}, \quad \mathbf{y} = \mathbf{C}\mathbf{x}$$

where definitions are given by the equations at the top of the page.

REFERENCES

[1] A. Nabae *et al.*, "A neutral-point-clamped PWM inverter," *IEEE Trans. Ind. Applicat.*, vol. IA-17, pp. 518–523, Sept./Oct. 1981.

[2] S. Ogasawara *et al.*, "Analysis of variation of neutral point potential in neutral-point-clamped voltage source PWM inverters," in *Conf. Rec. IEEE-IAS Annu. Meeting*, 1993, pp. 965–964.

[3] Y. Takahashi, *Systems and Control* Tokyo, Japan: Iwanami, 1978.

[4] S. Fukuda *et al.*, "Modeling and control of a neutral-point-clamped voltage source converter," in *Conf. Rec. IPEC-Yokohama*, 1995, pp. 470–475.

[5] Y. Iwaji *et al.*, "A parameter designing method of PWM voltage source rectifier," *Trans. Inst. Elect. Eng. Jpn.*, vol. 112-D, no. 7, pp. 639–647, 1992.

[6] S. Fukuda, "LQ control of sinusoidal current PWM rectifiers," *Proc. Inst. Elect. Eng.—Elect. Power Applicat.*, vol. 144, no. 2, pp. 95–100, 1997.

[7] A. Sagawa *et al.*, "A PWM control method of three level inverters for suppressing the neutral point potential variations," in *Conf. Rec. IEEJ-IAS Conf.*, 1993, pp. 315–356.

[8] M. Koyama *et al.*, "Space voltage vector-based new PWM method for large capacity three-level GTO inverter," in *Conf. Rec. IEEE IECON'92*, 1992, pp. 271–276.

[9] Y. Matsumoto *et al.*, "Neutral-point-potential control of an NPC converter," in *Conf. Rec. IEEJ-IAS Conf.*, 1996, vol. 3, pp. 369–372.

Shoji Fukuda (M'85–SM'96) received the M.E.E. and Ph.D. degrees from Hokkaido University, Sapporo, Japan, in 1967 and 1977, respectively.

From 1981 to 1983, he conducted research at the University of Saskatchewan, Saskatoon, Sask., Canada, as a Postdoctoral Fellow. He is currently an Associate Professor in the Division of Systems and Information, Graduate School of Engineering, Hokkaido University. He has been engaged in research on ac drives, microprocessor-based PWM control of rectifiers/inverters, and active power filters.

Dr. Fukuda is a member of the Institute of Electrical Engineers of Japan.

Yasumasa Matsumoto received the B.E.E. and M.E.E. degrees from Hokkaido University, Sapporo, Japan, in 1995, and 1997, respectively.

He joined Tohoku Electric Power Company Ltd., Mizusawa, Japan, in 1997 and is currently engaged in the maintenance of distribution lines at the Mizusawa Office.

Akira Sagawa received the B.E.E. and M.E.E. degrees from Hokkaido University, Sapporo, Japan, in 1993, and 1995, respectively.

He joined Hitachi Company Ltd. Mito Works, Hitachinaka, Japan, in 1995 and has been engaged in the design and development of traction systems for rolling stock.